Medeiros et al. 2012. *Int. J. Vehicle Structures & Systems*, 4(4), 141-147
ISSN: 0975-3060 (Print), 0975-3540 (Online)
doi: 10.4273/ijvss.4.4.05

International Journal of Vehicle Structures & Systems
Available online at www.ijvss.maftree.org

Numerical and Experimental Dynamic Analyses via Smart Composites

Ricardo de Medeiros[a,b], Marcelo L. Ribeiro[a], Gregório F. O. Ferreira[a], Flávio Donizeti Marques[a] and Volnei Tita[a]

[a]*Department of Aeronautical Engineering,*
São Carlos School of Engineering, University of São Paulo, Brazil.
[b]*Corresponding Author, Email: medeiros@sc.usp.br*

ABSTRACT:

This paper consists of evaluating a methodology based on a representative volume element and finite element analyses, using numerical and experimental modal analyses via smart composites. Vibration tests and finite element models are developed for aluminium cantilever beam with and without piezoelectric patches. The effective properties of the smart composites are calculated by applying the proposed methodology. Numerical predictions and experimental results are compared, showing that the relative differences between these dynamic analyses via piezoelectric patches are within 2.0%. The dynamic behaviour of the structure can be reasonably changed for a variation in the effective coefficients of the piezoelectric patches.

KEYWORDS:

Effective coefficients; Smart composites; Piezoelectric materials; Finite element analyses; Modal analyses

CITATION:

R. Medeiros, M.L. Ribeiro, G.F.O. Ferreira, F.D. Marques and V. Tita. 2012. Numerical and experimental dynamic analyses via smart composites, *Int. J. Vehicle Structures & Systems*, 4(4). 141-147. doi:10.4273/ijvss.4.4.05

1. Introduction

The materials in different forms can show a wide range of properties. However, only one material is not enough to provide a perfect balance of properties required for a specific application. In practice, it was discovered that a mixture of two or more materials, very often, can provide an advantageous properties combination. Thus, it is very important to develop a rigorous scientific methodology, which is capable of predicting the overall behaviour of heterogeneous media. This methodology provides a better material application. For this reason, many researchers have contributed to the development of a very important branch known as Mechanics of Composite Materials [1]. Considering, the current technological scenario, which seeks to reduce the number of components in the systems, especially in weight critical miniaturized systems, research in Mechanics of Composites Materials is very strategic. For this, intelligent devices capable for performing more than one function have been developed, often using an active material. These materials have been largely investigated during the last years [2].

Lead-Zirkonate-Titanate piezoelectric (PZT) materials have the property of converting electrical energy into mechanical energy, and vice versa [3]. The usage of these devices can reduce the weight, space and cost, depending on the application. This capability allows applications as sensors or as actuators in several industrial fields. For example, at the literature, it is possible to find scientific works on noise and vibration control, acoustic speakers, precision position control and structural health monitoring (SHM) [2]. Therefore, it can be concluded that the application requires the development of methodologies for calculating and predicting the behaviour and properties of smart materials. These methodologies must possess a high level of reliability and are often based on numerical, experimental, analytical and/or hybrid approaches. Several approaches have been considered to describe the electromechanical behaviour of the PZT coupling in smart composite materials. Frequently, authors have applied more than one approach to obtain reliable material coefficients and electromechanical behaviour evaluations [4]. Gaudenzi [6] obtained the electro-mechanical properties for PZT patches applied on metallic plates.

Poizat and Sester [7] showed how to assess two effective PZT coefficients (longitudinal and transverse). Petterman and Suresh [8] used unit cell models applied to piezo-composites. Azzouz et al [9] improved the formulation of a 3-noded aniso-parametric finite element (FE) to take into account the modelling of AFC (active fibre composite) and MFC (macro fibre composite). Paradies and Melnykowycz [10] studied the influence of inter-digital electrodes over mechanical properties of PZT fibres. After that, the research developed by Kar-Gupta and Venkatesh [11-13] investigated the influence of fibre distribution in PZT composites, considering both, fibre and matrix, with PZT properties. Berger et al [3, 14] evaluated PZT composites effective properties by comparing analytical and numerical techniques. However, until this moment, there is not a methodology, which is definitive. Thus, new scientific contributions using numerical analyses are necessary, mainly when experiments using PZT materials are required.

This paper consists of evaluating the methodology proposed by Medeiros et al [2, 5 and 15] using dynamic and experimental analyses via smart composites. This methodology is based on a Representative Volume Element and Finite Element Analysis (FEA) of smart composite materials. Firstly, computational models of a cantilever beam with PZT patches were developed using FE method. In order to determine the effective properties the PZT transducers (Midé QP10n), the methodology proposed by Medeiros et al [2, 5 and 15] was used. After that, an aluminium cantilever beam with two PZT patches attached at strategic positions was used. One patch is used to excite the structure. The other patch is used for data acquisition. In the test, a random signal was applied to the actuator and the output signal was measured by the sensor. Finally, combining the input and output signals, the Frequency Response Functions (FRFs) can be obtained from the FEA and experimental analyses. These FRFs are compared in order to evaluate the potential and limitation of the proposed methodology used to determine the effective coefficients of smart composites.

2. Material properties

The cantilever beam is made of aluminium type 7475 and the PZT patches are made of ceramic type Midé QP10n. The PZT wafer with epoxy matrix is covered with thin electrodes on the top and bottom sides. For the FE analyses, the material properties of the aluminium beam are obtained from the literature as follows: Elastic modulus = 69GPa, Poisson's ratio = 0.33 and density = 2697 kg/m^3. The effective properties for the PZT were calculated using the methodology proposed by Medeiros et al [2, 5 and 15] and are given in Table 1.

Table 1: Material Properties for the smart composite

Effective Coefficient	Value
c_{11}^{eff} (GPa)	81.73
c_{12}^{eff} (GPa)	5.23
c_{13}^{eff} (GPa)	50.06
c_{33}^{eff} (GPa)	46.35
c_{44}^{eff} (GPa)	5.91
c_{66}^{eff} (GPa)	5.63
e_{13}^{eff} (C/m^2)	-5.24
e_{15}^{eff} (C/m^2)	1.13
e_{33}^{eff} (C/m^2)	12.85
ε_{11}^{eff} (nF/m)	6.89
ε_{33}^{eff} (nF/m)	5.73
ρ (kg/m^3)	7400

The local coordinate system (1-2-3) for the composite material is defined by the fibre reinforcement (1), normal to the reinforcement (2) and normal to the plane of the layer (3). However, for the PZT patch, the local coordinate system axis (3) is related to the longitudinal direction of the fibres and 1- and 2-directions are related to the normal direction of the PZT patch. In this work, the polarization direction of PZT is aligned to the 3-direction.

3. FE model

First, a FE model based on a thin, rectangular and isotropic cantilever beam, as shown in Fig. 1, was developed and denoted as Model 1 (Fig. 2). The FE models for the aluminium beam were developed using 8-noded shell elements type S8 [16] with parabolic interpolation. Second, a FE model with two identical PZT patches mounted on the surface of the beam, as shown in Fig. 3, was carried out and denoted as Model 2 (Fig. 4). It is important to mention that the PZT patch close to the clamped support is used as actuator. The other PZT patch is used as sensor (Fig. 3). Also, the mechanical boundary conditions are applied in a strategic way on the beam in order to correctly represent the conditions provided by the real device.

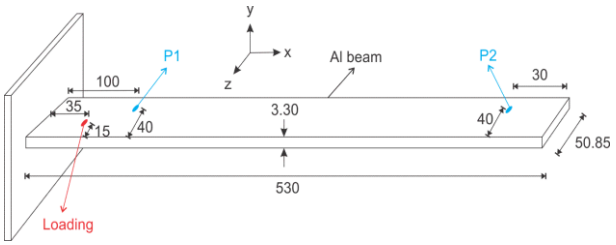

Fig. 1: Beam (mm) without PZT patches – Model 1

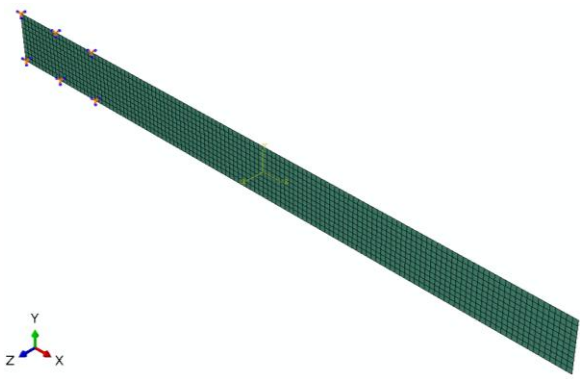

Fig. 2: FE model of beam without PZT patches – Model 1

Regarding Model 2, the homogenized PZT transducers have the following dimensions 50.8 × 25.4 × 0.5 mm. They were modelled using 20-noded solid elements type C3D20E [16] with parabolic interpolation. Each node gives displacements in x, y and z directions and electric voltage [16]. Therefore, the electric potential was measured in a specific node of the model on the free surface that corresponds to local information for an applied strain. In practice, the free surface of each PZT patch is covered with an electrode, which ensures a uniform level of induced electric potential (equi-potential) in the free surface of the patch. In order to ensure perfect bonding between the PZT patch and the beam, the nodes on the bottom surface of the PZT patch is coupled to the surface of the beam, using the "tie" contact [16]. The grounding of nodes of the PZT surfaces attached to the beam is set as zero potential at any stage of strain. The purpose of grounding consists of defining a reference value.

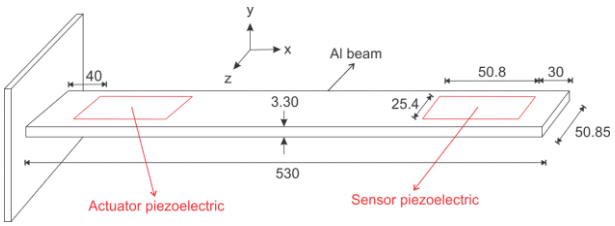

Fig. 3: Beam (mm) with PZT patches – Model 2

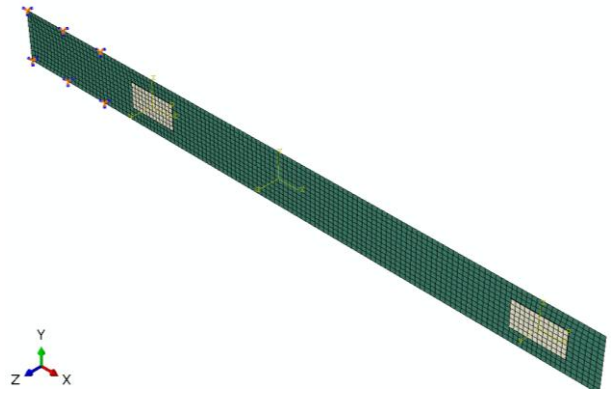

Fig. 4: FE model of beam with PZT patches – Model 2

Another important aspect is to ensure the mechanical coupling between the beam and the PZT transducer. Once the mechanical coupling is assured, it is necessary to define appropriate conditions for reading the electric potential from the PZT patches. Naturally, the dielectric properties of the Midé QP10n prevent the homogeneous distribution of the induced electrical charges on the free surface of the patch. Thus, Open-Circuit (OC) and Short-Circuit (SC) electrical boundary conditions can be considered. For OC, all nodes of the PZT patch surface attached to the beam are considered electrically grounded and the free respect to equi-potential condition. For SC, the nodes of the top and the bottom surfaces of the patch are grounded so that the electrical potentials at the top and the bottom of each PZT patch are maintained constants. The smart composite behaves as a SC device. Physically, the generated surface charges are disposed outside the PZT patch by conductive wires [17].

The dynamic FE simulations consist of performing modal analyses followed by below procedures:

- Model 1: A perpendicular loading is applied on the beam. The results are obtained from the nodes where accelerometers are attached during experimental tests (positions P1 & P2 as in Fig. 1).
- Model 2: Harmonic electrical potential is applied at the PZT actuator. The output measurements are obtained from the PZT sensor. This harmonic input is electric potential difference with format as a sine wave with amplitude from 100V to -100V. The frequency of the sinusoidal electrical potential is applied at an interval of 0-600Hz in steps of 0.5Hz.

Based on the input and output signals, numerical FRFs are obtained from the results of FE models 1 and 2.

4. Results and discussions

The first experimental analysis consists of verifying the prediction quality for a cantilever beam without PZT patches (Model 1). Fig. 5 shows the entire setup of experimental modal testing. An impact hammer is used to apply an impulse input in the beam near the clamped region. The output signal is captured by accelerometers attached at positions P1 and P2 (see Fig. 1). The acquisition frequency is applied at an interval of 0-600Hz in steps of 0.5Hz. Based on the input and output signals, the experimental FRF of the beam is obtained.

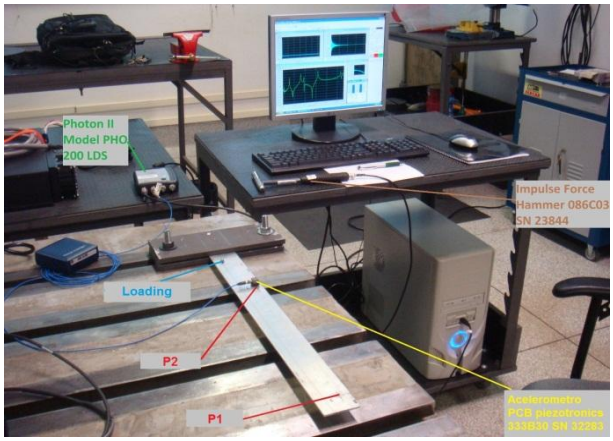

Fig. 5: Test setup of the beam without PZT patches

The results for aluminium beam without PZT patches (Model 1) are shown in Figs. 6 and 7 respectively for the locations P1 and P2. The experimental and numerical FRFs correlate well. The maximum difference between the numerical and experimental results is within 3%. Difference is justified due to some factors such as real and applied boundary conditions in the model, uncertainties related to the properties of the aluminium beam and damping effects, which are disregarded in the FE simulations.

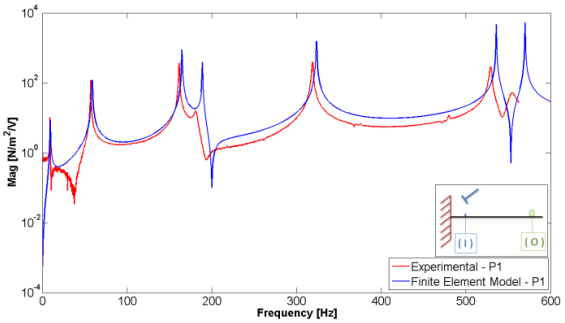

Fig. 6: FRF of the beam without PZT patch – P1.

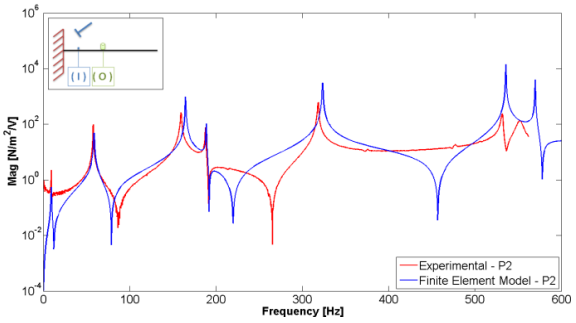

Fig. 7: FRF of the beam without PZT patch – P2.

The second experimental analysis consists of comparing the FRF obtained experimentally to the numerical predictions for a cantilever beam with PZT patches (Model 2). Figs. 8 and 9 show a schematic

representation and the actual test setup respectively for the cantilever beam with PZT patches. For this case, the influence of effective coefficients for the PZT material is investigated to evaluate the methodology proposed by Medeiros et al [2, 5 and 15]. A random signal was applied to the PZT actuator. The output measurements were obtained by the PZT sensor. The frequency is applied at an interval 0-600Hz in steps of 0.5Hz. The experimental FRF is obtained based on the input and output signals.

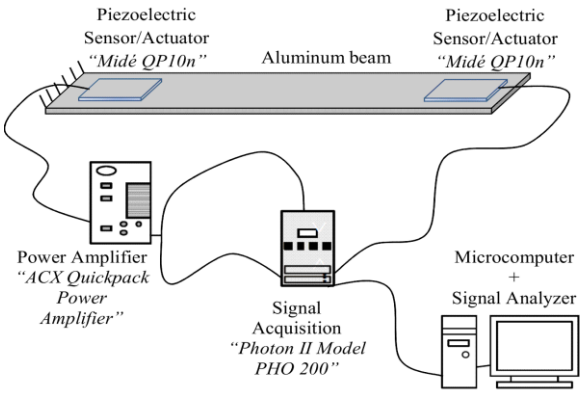

Fig. 8: Schematic setup for the beam with PZT patches

Fig. 9: Test setup for the beam with PZT patches

The harmonic analysis results for Model 2 are shown in Fig.10. The experimental FRF presents some noise for the frequency between 0 and 100Hz. Such low noise does not influence the behaviour of the beam. The differences between the numerical and experimental results can be explained by the absence of damping effects in the FE simulations, the boundary conditions applied in the model and uncertainties related to the material properties of the beam and PZT patches.

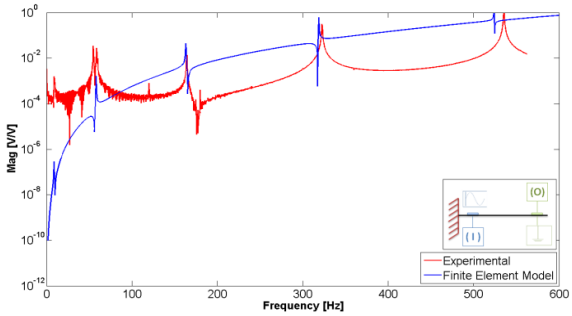

Fig. 10: FRF of cantilever beam with PZT patches

Figs.11 to 18 show the first 8 mode shapes from the dynamic analysis for the cantilever beam with two PZT patches. The first, second, fourth, sixth and seventh modes are bending shapes. The third mode is in-plane shape. The fifth and eighth modes are torsion shapes.

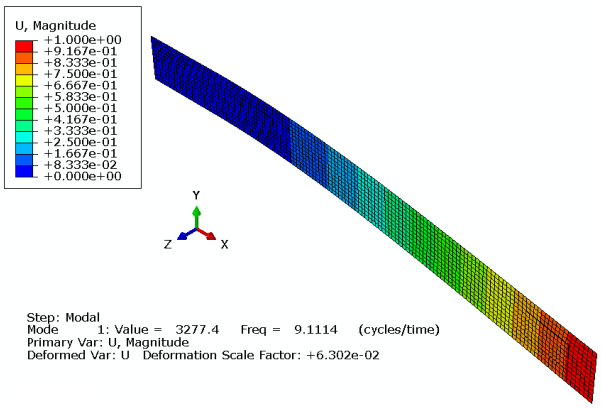

Fig. 11: Mode 1 for the beam with PZT patches

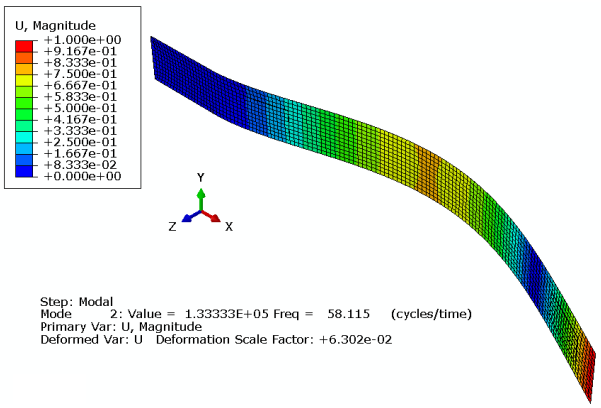

Fig. 12: Mode 2 for the beam with PZT patches

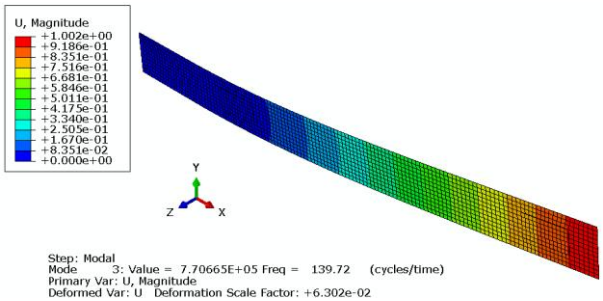

Fig. 13: Mode 3 for the beam with PZT patches

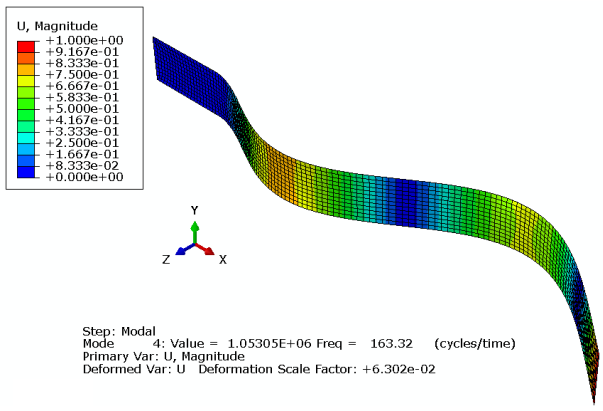

Fig. 14: Mode 4 for the beam with PZT patches

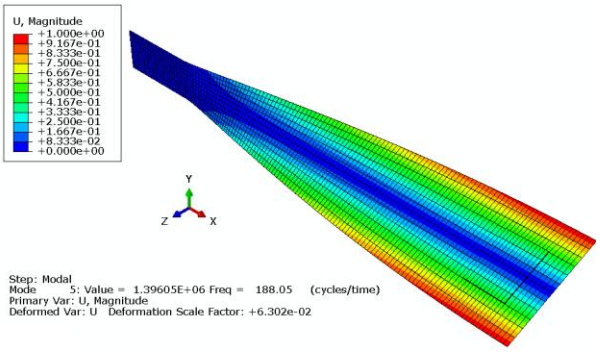

Fig. 15: Mode 5 for the beam with PZT patches

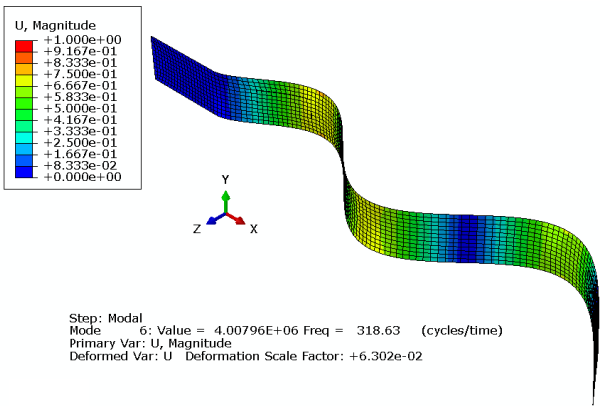

Fig. 16: Mode 6 for the beam with PZT patches

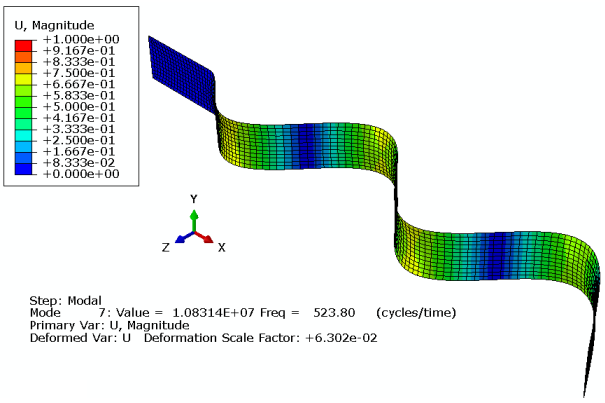

Fig. 17: Mode 7 for the beam with PZT patches

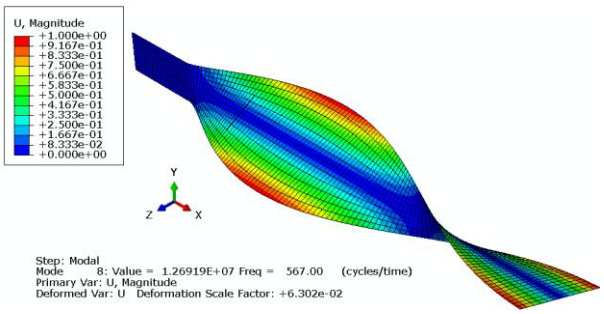

Fig. 18: Mode 8 for the beam with PZT patches

Table 2 shows the comparison between natural frequencies obtained by the tests and FE analyses. The relative difference (RD) between the two results is within 2%. These results show the capability of the FE model to predict the dynamic behaviour of the structure via PZT patches. Thus, the potential of the methodology applied to determine the properties of the smart composites was verified.

Table 2: Modal frequencies of cantilever beam with PZT patches: Experimental vs. FE results

Mode	Test Freq. (Hz)	FEA Freq. (Hz)	Rel. Diff. (%)
f_1	9.06	9.01	0.55%
f_2	58.75	58.05	1.19%
f_3	-	-	-
f_4	164.37	163.14	0.75%
f_5	-	-	-
f_6	322.51	318.84	1.14%
f_7	535.68	523.93	2.19%

The third experimental analysis consists of performing tests considering the PZT in OC to verify the influence of the stiffness and the mass of PZT patches in the behaviour of the beam. An impact hammer is used to apply a sinusoidal impulse input of 1N near the clamped region of the beam. The output signal is captured by accelerometers attached at positions P1 and P2, likewise performed in the first analysis. Figs. 19 to 22 show that the FRF amplitudes and phase angles from third test results are quite similar. Table 3 shows the natural frequencies for the beam with and without PZT patches in OC obtained by experimental analyses. The relative differences are within 2.2%. This demonstrates that the PZT patches have low influence on the natural frequencies of the structure.

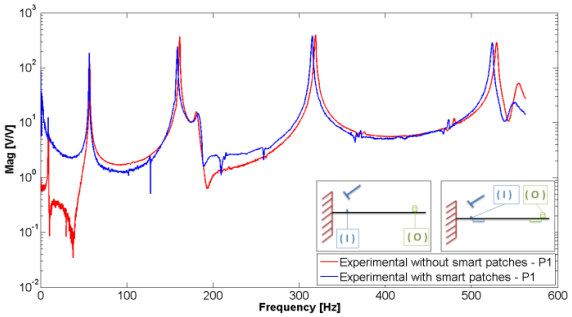

Fig. 19: FRF of beam with & without PZT patches in OC – P1

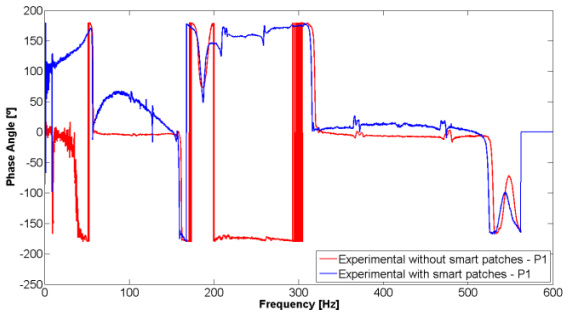

Fig. 20: Phase of beam with & without PZT patches in OC – P1

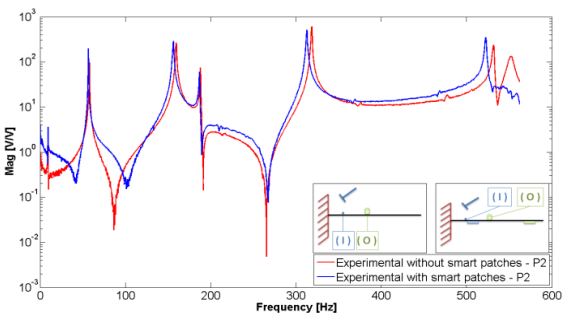

Fig. 21: FRF of beam with & without PZT patches in OC – P2

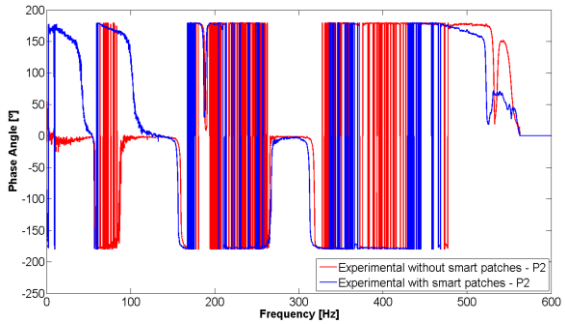

Fig. 22: Phase of beam with & without PZT patches in OC – P2

Table 3: Experimental modal frequencies for the beam with & without PZT patches in OC – P1 & P2

Type	Without PZT P1	With PZT P1	Rel. Diff.
f_1 (Hz)	9.06	8.91	1.66%
f_2 (Hz)	57.19	56.56	1.10%
f_3 (Hz)	-	-	-
f_4 (Hz)	161.56	158.91	1.64%
f_5 (Hz)	181.38	183.00	0.89%
f_6 (Hz)	319.10	315.31	1.19%
f_7 (Hz)	529.22	524.26	0.94%
Type	Without PZT P2	With PZT P2	Rel. Diff.
f_1 (Hz)	9.37	9.22	1.60%
f_2 (Hz)	57.97	56.72	2.16%
f_3 (Hz)	-	-	-
f_4 (Hz)	159.68	156.36	2.08%
f_5 (Hz)	188.12	186.87	0.66%
f_6 (Hz)	318.63	312.82	1.82%
f_7 (Hz)	531.62	522.71	1.68%

Finally, the influence of variation in the effective coefficients in the numerical predictions is investigated. For this study, an artificial "error" as a factor of 100 and 100 for the previously calculated values is introduced in the numerical analyses. It can be seen from Fig. 23, Tables 4 and 5 that these variations in the PZT coefficients produce high variations in the dynamic responses of the system.

Table 3: Influence of PZT effective coefficients variation on the natural frequencies of the beam with PZT patches

Type	Exp.	FE simulation		
		x1	x10	x100
f_1 (Hz)	9.06	9.01	9.01	9.01
f_2 (Hz)	58.75	58.05	58.05	58.55
f_3 (Hz)	-	-	-	-
f_4 (Hz)	164.37	163.14	163.01	163.66
f_5 (Hz)	-	-	-	-
f_6 (Hz)	322.51	318.84	318.35	320.83
f_7 (Hz)	535.68	523.93	522.93	531.42

Table 4: Influence of PZT effective coefficients variation on the maximum amplitudes for the beam with PZT patches

Type	Exp.	FE simulation		
		1x	10x	100x
A_1 (V/V)	1.584E-03	6.771E-18	7.838E-19	1.215E-20
A_2 (V/V)	2.877E-02	3.907E-14	5.462E-15	1.135E-16
A_3 (V/V)	-	-	-	-
A_4 (V/V)	1.367E-02	1.054E-12	1.273E-13	3.544E-14
A_5 (V/V)	-	-	-	-
A_6 (V/V)	3.157E-01	1.448E-11	8.613E-13	2.097E-14
A_7 (V/V)	1.012E00	2.381E-11	2.146E-12	2.287E-12

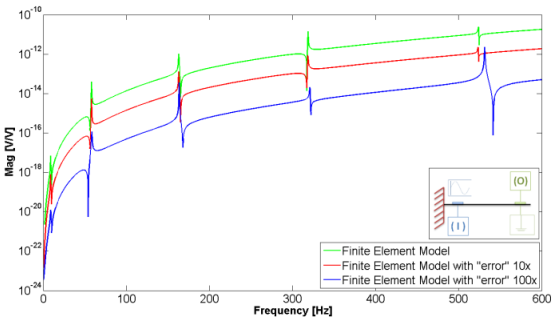

Fig. 23: Influence of PZT effective coefficients variation on the FRF of the beam with PZT patches

5. Conclusions

The methodology proposed by Medeiros et al. [2, 5 and 15] applied to determine the effective properties of the smart composites were evaluated using FE and experimental dynamic analyses. Based on the presented results, it is concluded that this methodology is a suitable alternative to determine effective coefficients for smart composite materials. Different comparisons between FE and experimental dynamic analysis results show good agreement. The relative differences between the analyses via smart composites were within 2%. Therefore, the FE models developed in this work can be used to predict the dynamic behaviour of the beams via PZT patches.

ACKNOWLEDGEMENTS:

The authors are thankful to FAPESP (Process Nos.: 2012/01047-8 and 2009/00544-5), CNPq (Process No.: 135652/2009-0) and FAPEMIG for partially funding the present research work through INCT-EIE. The authors also would like to thank Prof. Reginaldo Teixeira Coelho from Engineering School of São Carlos, University of São Paulo for the ABAQUS license.

REFERENCES:

[1] J.B. Castillero, J.A. Otero and R.R. Ramos. 1998. Asymptotic homogenization of laminated piezocomposite materials, *Int. J. Solids & Structures*, 35(5-6), 527-541. http://dx.doi.org/10.1016/S0020-7683(97)00028-0

[2] R. Medeiros, M.E. Moreno, F.D. Marques and V. Tita. 2012. Effective properties evaluation for smart composite materials, *J. Brazilian Society of Mechanical Sciences and Engineering*, 34, 362-370. http://dx.doi.org/10.1590/S1678-58782012000500004

[3] H. Berger, S. Kari, U. Gabbert, R.R. Ramos, R. Guinovart, J.A. Otero and J.B. Castillero. 2005. An analytical and numerical approach for calculating effective material coefficients of piezoelectric fiber composites, *Int. J. Solids & Structures*, 42(21-22), 5692-5714. http://dx.doi.org/10.1016/j.ijsolstr.2005.03.016

[4] M.E. Moreno, V. Tita and F.D. Marques. 2009. Finite element analysis applied to evaluation of effective material coefficients for piezoelectric fiber composites, *Proc. Brazilian Symp. Aerospace Eng. & Applications*, São Paulo, Brazil.

[5] R. Medeiros, M.E. Moreno, V. Tita, F. D. Marques and M. Sartorato. 2010. Electromechanical response of 1-3 piezoelectric fiber composites: A unit cell approach for numerical evaluation of effective properties, *Proc. Sixth*

National Cong. Mechanical Engineering, Campina Grande, Paraíba, Brazil.

[6] P. Gaudenzi. 1997. On the electro mechanical response of active composite materials with piezoelectric inclusions, *Computers & Structures*, 65(2), 157-168. http://dx.doi.org/10.1016/S0045-7949(96)00375-6

[7] C. Poizat and M. Sester. 1999. Effective properties of composites with embedded piezoelectric fibres, *Computational Materials Science*, 16(1-4), 89-97. http://dx.doi.org/10.1016/S0927-0256(99)00050-6

[8] H.E. Pettermann and S. Suresh. 2000. A comprehensive unit cell model: a study of coupled effects in piezoelectric 1-3 composites, *Int. J. Solids and Structures*, 37(39), 5447-5464. http://dx.doi.org/10.1016/S0020-7683(99)00224-3

[9] M.S. Azzouz, C. Mei, J.S. Bevan and J.J. Ro. 2001. Finite element modeling of MFC/AFC actuators and performance of MFC, *J. Intelligent Material Systems and Structures*, 12(9), 601-612. http://dx.doi.org/10.1177/10453890122145384

[10] R. Paradies and M. Melnykowycz. 2007. Numerical stress investigation for piezoelectric elements with circular cross section and interdigitated electrodes, *J. Intelligent Material Systems and Structures*, 18(9), 963-972. http://dx.doi.org/10.1177/1045389X06071438

[11] R. Kar-Gupta and T.A. Venkatesh. 2005. Electromechanical response of 1-3 piezoelectric composites: effect of poling characteristics, *J. Applied Physics*, 98(5), 054102. http://dx.doi.org/10.1063/1.2014933

[12] R. Kar-Gupta and T.A. Venkatesh. 2007. Electromechanical response of 1-3 piezoelectric composites: An analytical model, *Acta Materialia*, 55(3), 1093-1108. http://dx.doi.org/10.1016/j.actamat.2006.09.023

[13] R. Kar-Gupta and T.A. Venkatesh. 2007. Electromechanical response of 1-3 piezoelectric composites: A numerical model to assess the effects of fiber distribution. *Acta Materialia*, 55(4), 1275-1292. http://dx.doi.org/10.1016/j.actamat.2006.09.042

[14] H. Berger, S. Kari, U. Gabbert, R.R. Ramos, J.B. Castillero, R. Guinovart-Diaz, F.J. Sabina and G.A. Maugin. 2006. Unit cell models of piezoelectric fiber composites for numerical and analytical calculation of effective properties, *Smart Materials and Structures*, 15(2), 451-458. http://dx.doi.org/10.1088/0964-1726/15/2/026

[15] R.R. Ramos, R. Medeiros, R.G. Díaz, J.B. Castillero, J.A. Otero and V. Tita. 2013. Different approaches for calculating the effective elastic properties in composite materials under imperfect contact adherence, *Composite Structures*, 99, 264-275. http://dx.doi.org/10.1016/j.compstruct.2012.11.040

[16] *Abaqus Documentation*, Version 6.10-1, 2010, Dassault Systèmes, USA.

[17] C.C. Pagani Jr and M. A. Trindade. 2009. Optimization of modal filters based on arrays of piezoelectric sensors, *Smart Materials and Structures*, 18(9), 095046. http://dx.doi.org/10.1088/0964-1726/18/9/095046